

SUPPLEMENTAL INFORMATION

# Concentrations, gas-particle distributions, and source indicator analysis of brominated flame retardants in air at Toolik Lake, Arctic Alaska

*Cleo L. Davie-Martin,<sup>1,4</sup> Kimberly J. Hageman,<sup>\*,1</sup> Yu-Ping Chin,<sup>2</sup> Benjamin J. Nistor,<sup>1</sup> Hayley Hung<sup>3</sup>*

<sup>1</sup> Department of Chemistry, University of Otago, Dunedin 9016, New Zealand

<sup>2</sup> School of Earth Sciences, The Ohio State University, Columbus, Ohio 43210, United States<sup>3</sup>  
Air Quality Processes Research Section, Environment and Climate Change Canada, Toronto, Ontario M3H 5T4, Canada

### **Present Address**

<sup>4</sup> Department of Environmental and Molecular Toxicology, Oregon State University, Corvallis, Oregon 97331, United States

### **Corresponding Author**

\* To whom correspondence should be addressed

E-mail: khageman@chemistry.otago.ac.nz

Telephone: +64-3-479-5214

Fax: +64-3-479-7906

### **Summary:**

Supporting information contains 35 pages, including 10 tables and 11 figures.

## Table of Contents

<b>Section 1</b>	Details of the flow-through air sampler calibration for calculation of sample volumes.	S3
<b>Figure S1</b>	Flow-through sampler set up for field calibration.	S3
<b>Figure S2</b>	Relationship between ‘internal’ and ‘external’ wind speeds for calibration of the flow-through air samplers.	S4
<b>Table S1</b>	Total air volumes sampled with flow-through air samplers.	S5
<b>Section 2</b>	Details of the chemicals, sample preparation, and analytical procedures.	S5
<b>Table S2</b>	GC-MS retention times, quantification, and confirmation ions for BFRs in ECNI.	S8
<b>Section 3</b>	Recommendations for the analysis of BDE-209.	S8
<b>Figure S3</b>	Comparison of total ion chromatograms for a BFR standard run under the same conditions using a standard single-tapered gooseneck splitless liner and a drilled uniliner for direct injections.	S8
<b>Section 4</b>	Details of the quality control measures.	S10
<b>Figure S4</b>	Extraction method recoveries for high-volume and flow-through air sampling media.	S11
<b>Table S3</b>	Estimated detection limits for high-volume and flow-through air sampling media.	S12
<b>Table S4</b>	Average concentrations of target BFRs used for field-blank subtractions with the high-volume and flow-through air sampling media.	S13
<b>Table S5</b>	Summary of average 24-hour meteorological data during the 60-day sampling period at Toolik Field Station.	S15
<b>Figure S5</b>	Wind roses illustrating wind frequency data during each 2-day high-volume air sample.	S17
<b>Table S6</b>	Gas-phase concentrations ( $\text{pg m}^{-3}$ ) of target BFRs measured in high-volume air samples at Toolik Lake, Alaska.	S19
<b>Table S7</b>	Particle-bound concentrations ( $\text{pg m}^{-3}$ ) of target BFRs measured in high-volume air samples at Toolik Lake, Alaska.	S21
<b>Table S8</b>	Total concentrations ( $\text{pg m}^{-3}$ ) of target BFRs measured in high-volume air samples at Toolik Lake, Alaska.	S22
<b>Figure S6</b>	Frequency of detection for target BFRs in high-volume air sampling media.	S25
<b>Table S9</b>	Compilation of BFR concentrations in air reported at other Arctic sites.	S26
<b>Figure S7</b>	BFR profiles (combined gas- and atmospheric particle-bound phases) during the 60-d sampling period.	S28
<b>Figure S8</b>	Relationship between BFR concentrations in air and the wind source indicators.	S29
<b>Figure S9</b>	Relationship between the natural logarithm of BFR concentrations in air and the inverse of 48-hour local air temperature observations.	S30
<b>Figure S10</b>	Correlations between $\log K_p$ and the inverse of temperature for selected BFRs.	S31
<b>Table S10</b>	Total concentrations ( $\text{pg m}^{-3}$ ) of target BFRs measured in flow-through air samples at Toolik Lake, Imnavait Creek, and Oksrukuyik Creek.	S32
<b>Figure S11</b>	Frequency of detection for target BFRs in flow-through air sampling media.	S33
<b>Section 5</b>	References	S34

## Section 1. Details of the flow-through air sampler calibration for calculation of sample volumes.

### *Flow-through sampler calibration*

An AM4217SD Lutron anemometer (Jaycar Electronics, Dunedin, New Zealand) was mounted inside the tail pipe of the flow-through sampler (FTS) and co-deployed with comprehensive WS-2083 weather stations (Scientific Sales, New Zealand; Ambient Weather, Chandler, AZ) on a tripod supporting the flow-through air samplers 2.5 m above the roof of the University of Otago Science II building (55 m agl) (Figure S1). The weather station collected data every 45 s and logged the average values over 5-min periods. The FTS was positioned on a bearing mount so that it could turn through 360° to replicate field conditions and account for the time taken for the sampler to turn into the wind when it shifts direction. Low-density PUF plugs (5x1" plugs, 95 mm diameter, NZ Foam Distributors, New Zealand) were installed in the FTS cartridge so that the relationship between external and internal wind speed could be determined. 957 observations were logged between the 28-30<sup>th</sup> July and 11-13<sup>th</sup> August, 2015. Internal wind speeds were measured at 10-s intervals and averaged over 5-min intervals corresponding to those of the weather stations. From these observations a calibration curve representing the relationship between the internal and external wind speeds was determined (Figure S2). A quadratic equation provided the best fit for these observations (eq S1) and was used to calculate the volume of air sampled.



**Figure S1.** Flow-through sampler set up for field calibration on the Science II Building roof at the University of Otago, Dunedin, New Zealand.

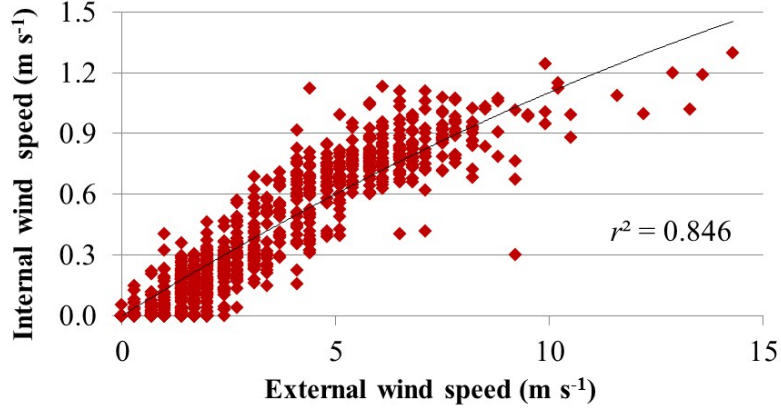


**Figure S2.** Relationship between ‘internal’ and ‘external’ wind speeds determined during field calibration of the flow-through air samplers.

$$U_{\text{internal}} = -0.002 \cdot U_{\text{external}}^2 + 0.130 \cdot U_{\text{external}} \quad (\text{S1})$$

*Calculation of the volume of air sampled*

The volume of air actively sampled by the FTS was calculated using eq S2:<sup>1</sup>

$$V = U_{\text{internal}} \cdot \pi \cdot r^2 \cdot t \quad (\text{S2})$$

where  $V$  is the volume of air sampled ( $\text{m}^3$ ),  $U_{\text{internal}}$  is the wind speed inside the sampler ( $\text{m s}^{-1}$ ),  $r$  is the radius of the FTS tailpipe (0.0465 m), and  $t$  is the sampling period of each measurement (300 s). Sample volumes were calculated for each 5-min interval and summed to obtain the total volume of air actively sampled during each 18-d sampling period (Table S1). Additionally, the FTS will also passively sample via diffusion, which becomes increasingly important during calm periods. Previous studies suggest that traditional polyurethane foam samplers can sample on the order of 1.8-9.3  $\text{m}^3$  per day, depending on the chemical.<sup>2, 3</sup> Thus, using the reported mean value of 3.9  $\text{m}^3$ ,<sup>1</sup> we estimated that during our 18-d sampling periods, diffusion-based sampling equated to 70.2  $\text{m}^3$ , which contributed between 1.5-2.5% of the total air volume sampled (Table S1).

**Table S1.** Total volumes of air sampled during each FTS period, including the contributions from active (wind-driven) and passive (diffusion-based) sampling.

Sample location	Sample period	% active sampling	% passive sampling	Total volume of air sampled ( $\text{m}^3$ )
Toolik Lake (0 km)	A (6-24 <sup>th</sup> Jul)	98.0	2.0	3430
	B (24 <sup>th</sup> Jul-11 <sup>th</sup> Aug)	98.3	1.7	4210
	C (11-29 <sup>th</sup> Aug)	97.8	2.2	3240
Imnavait Creek (~10 km)	A (6-24 <sup>th</sup> Jul)	97.8	2.2	3200
	B (24 <sup>th</sup> Jul-11 <sup>th</sup> Aug)	98.5	1.5	4680
	C (11-29 <sup>th</sup> Aug)	97.5	2.5	2860
Oksrukuyik Creek (~20 km)	A (6-24 <sup>th</sup> Jul)	98.0	2.0	3440
	B (24 <sup>th</sup> Jul-11 <sup>th</sup> Aug)	98.5	1.5	4630
	C (11-29 <sup>th</sup> Aug)	97.9	2.1	3410

## Section 2. Details of the chemicals, sample preparation, and analytical procedures.

### *Chemicals*

High purity pesticide grade solvents, including acetone (>99%), dichloromethane (>99%), ethyl acetate (>99%), and *n*-hexane (>98%) were obtained from Merck (Darmstadt, Germany). Florisil (activated magnesium silicate) (60/100 mesh) was obtained from Restek (Bellefonte, PA) and acid-washed sand was purchased from VWR (Leuven, Belgium). 30-mm glass fiber filters were obtained from Munktell (Bärentstein, Germany).

Fourteen brominated flame retardants were purchased as individual standards from Wellington Laboratories Inc. (Ontario, Canada): 2,2',4-tribromodiphenyl ether (BDE-17), 2,4,4'-tribromodiphenyl ether (BDE-28), 2,2',4,4'-tetrabromodiphenyl ether (BDE-47), 2,3',4,4'-tetrabromodiphenyl ether (BDE-66), 2,3',4',6-tetrabromodiphenyl ether (BDE-71), 2,2',3,4,4'-pentabromodiphenyl ether (BDE-85), 2,2',4,4',5-pentabromodiphenyl ether (BDE-99), 2,2',4,4',6-pentabromodiphenyl ether (BDE-100), 2,2',3,4,4',5'-hexabromodiphenyl ether (BDE-138), 2,2',4,4',5,5'-hexabromodiphenyl ether (BDE-153), 2,2',4,4',5,6'-hexabromodiphenyl ether (BDE-154), 2,2',3,4,4',5',6-heptabromodiphenyl ether (BDE-183), decabromodiphenyl ether (BDE-209), and 1,2-bis(2,4,6-tribromophenoxy)ethane (BTBPE, Firemaster 680). An isotopically labelled polychlorinated biphenyl, <sup>13</sup>C<sub>12</sub>-PCB-178 (>98%), was obtained from CDN Isotopes (Pointe-Claire, Quebec, Canada).

### *Preparation of experimental and sampling equipment*

Florisil and acid-washed sand were pre-cleaned by baking at 400 °C for 4 h prior to use. Additionally, all experimental equipment was washed in warm soapy water then rinsed thoroughly with tap water and distilled water prior to use. All glassware and metalware were then baked at 400 °C for 4 h. Any equipment that could not be baked was instead solvent rinsed or sonicated (5-min per solvent) with acetone, ethyl acetate, and *n*-hexane and left to evaporate in the fumehood for 20 min prior to use. Quartz fiber filters (QFF) (100 mm diameter, Munktell, NZ) were baked in individual aluminum foil packets for 4 h at 400 °C and stored until deployment. All 1" (2.54 cm) and 3" (7.62 cm) high-volume air sampling polyurethane foam (PUF) plugs (60 mm diameter, Tisch, Cleves, OH) were pre-cleaned with pressurized liquid extraction (PLE) using an Accelerated Solvent Extractor 300 System (Dionex, Sunnyvale, CA). Three separate extractions with 75:25 hexane:acetone, 90:10 hexane:acetone, and 100% hexane were used with the following conditions: 5-min heat time, 5-min static time, 1 static cycle, 100% flush volume, 240-s purge time, 1500 psi, and 75 °C. Residual solvents in the PUF plugs were left to evaporate in the fumehood overnight before being stored in pre-cleaned glass cartridges (Tisch, Cleves, OH) and wrapped in pre-baked aluminum foil packets until deployment. The low-density PUF plugs (95 mm diameter, NZ Foam Distributors, New Zealand), used for flow-through air sampling, were pre-cleaned using the same conditions outlined above, except that a 60-s purge time was selected and different solvent combinations were utilized, including two extractions with 90:10 hexane:acetone and a final extraction with 100% hexane. Following evaporation of residual solvents, the low-density PUF plugs were stored in pre-cleaned aluminum sample cartridges with Teflon-lined lids until deployment.

### *Sample extraction*

Samples were kept frozen until extraction and analysis, except during the 15-day transport between Toolik Field Station and Dunedin, New Zealand. BFRs were extracted from PUF and QFFs using PLE and prior to extraction, all samples were spiked with an isotopically labelled polychlorinated biphenyl surrogate (<sup>13</sup>C<sub>12</sub>-PCB-178) to account for potential losses of target analytes during sample work-up. We used a labelled PCB surrogate because it has a similar structure and extraction efficiency to the PBDEs but does not interfere with the PBDE quantification

ions.<sup>4</sup> Previous studies also use labelled and unlabeled PCBs as surrogates for PBDE analysis.<sup>4,7</sup> Two day high-volume air PUF samples were packed into 34-mL stainless steel extractions cells and extracted with 75:25 hexane:acetone using the following conditions: 5-min heat time, 5-min static time, 2 static cycles, 100% flush volume, 240-s purge time, 1500 psi, and 100 °C. For 10% of the high-volume PUF samples, 5 g of Florisil was included downstream of the PUF in the extraction cell (i.e., in-cell cleanup<sup>8</sup>) in an attempt to retain matrix components and minimize sample clean-up. However, we found that Florisil was not effective at removing sufficient quantities of the matrix components and additional external clean-up was required whether Florisil was present or not. Thus, the remaining samples were extracted without in-cell clean-up. When the sample PUF (3" plug) and breakthrough PUF (1" plug) had been stored together, both were combined and extracted together as a single sample. When the breakthrough PUF had been stored separately (i.e., once in every 6-d period), the 1" plugs were extracted using the same method as described above, except that baked, acid-washed sand was used to fill the dead volume in the cell and was topped with a 30-mm glass fiber-filter (GFF) to prevent sand causing blockages in the fluidic pathway.

High-volume QFF samples were packed into 34-mL stainless steel extraction cells and topped with pre-baked, acid-washed sand to fill the dead volume and a 30-mm GFF. The cells were first extracted with 50:50 hexane:acetone, followed by a second extraction with 100% hexane. Both extractions used the following conditions: 5-min heat time, 5-min static time, 3 static cycles, 100% flush volume, 240-s purge time, 1500 psi, and 100 °C.

Flow-through air PUF samples were extracted with 90:10 hexane:acetone using the following conditions: 5-min heat time, 5-min static time, 3 static cycles, 100% flush volume, 240-s purge time, 1500 psi, and 75 °C. Only two of the 1" PUF plugs would fit in each 100-mL extraction cell and as such, each sample (4x1" PUF) was extracted in two separate cells and the extracts combined. For all samples, the storage jars were solvent rinsed once each with acetone and hexane to remove any BFRs that may have adsorbed to the surfaces during storage, and combined with their corresponding sample extracts.

#### *Sample clean-up*

High-volume air sample extracts were slightly colored and produced chromatograms that contained a handful of high-abundance, non-target peaks, which indicated that further clean-up procedures were required. We believe the samples were heavily impacted by particulate matter from sources at the field station itself (e.g., the wood-burning sauna, evening bonfires, and the waste incinerator) and from dust picked up through the operation of heavy machinery and construction occurring on the nearby Dalton Highway throughout the summer. Thus, two high-volume air samples (QFF + PUF for the period of 6-9<sup>th</sup> July 2013) were sacrificed to develop a clean-up method that would allow for removal of the majority of the co-extracted matrix components in the samples. The low-density PUF used in the flow-through air samplers contained a strongly colored yellow pigment and as a result, the flow-through air samples also required additional external clean-up.

Gel permeation chromatography (GPC) with a Dionex UltiMate-3000 Series high performance liquid chromatography (HPLC) system with a variable wavelength detector (VWD-3400) (Germering, Germany) coupled to a Teledyne ISCO Foxy 200 fraction collector (Lincoln, NE) was used for size-based sample fractionation. A 25-mm PLgel Prep guard column and 25-mm preparatory PL Prep column (450 mm in length), each comprised of a styrene divinylbenzene copolymer stationary phase, were aligned in series for the separations. Dichloromethane was used as the mobile phase at a flow rate of 6 mL min<sup>-1</sup>. The UV-vis detector was operated in single wavelength detection mode with a wavelength of 254 nm. At the beginning of each day, a standard containing the target BFRs and isotopically labelled surrogate PCB was run to determine the cut-off time for sample fractionation (23.7 min). Prior to the cut-off time, the portion of the sample containing matrix components was directed to waste and after

which, the fraction containing the target BFRs was collected in a pre-cleaned glass sampling bottle. Each sample required a total run time of 32 min. Following GPC, the collected fraction containing the target BFRs was solvent exchanged to ethyl acetate and concentrated to 300  $\mu\text{L}$  under a constant stream of nitrogen (Zymark Turbovap II, Hopkington, MA).

#### *Analysis with gas chromatography*

All extracts were analyzed on an Agilent 6890N gas chromatograph coupled to an Agilent 5957 mass selective detector (GC-MS) (Santa Clara, CA). An Agilent 7683B autosampler was used to inject 1  $\mu\text{L}$  of sample extract into the split/splitless inlet. An Agilent DB-5MS column designed specifically for the analysis of PBDEs (15 m length x 250  $\mu\text{m}$  internal diameter x 0.1  $\mu\text{m}$  film thickness) was used for the chromatographic separations, with helium as the carrier gas at a flow rate of 1.5  $\text{mL min}^{-1}$  with a solvent delay of 4.7 min. A Restek drilled uniliner with the hole at the top (specifically designed for modifying *electronic pneumatics control*, EPC, split/splitless inlet systems to allow for direct injections) was installed in the inlet and formed a direct connection with the head of the column. The inlet was used in pulsed splitless mode (25 psi until 1 min) at a temperature of 325  $^{\circ}\text{C}$  and the MS transfer line started at a temperature of 310  $^{\circ}\text{C}$ , was held for 17 min, and then ramped at 15  $^{\circ}\text{C min}^{-1}$  to 325  $^{\circ}\text{C}$  with a final hold of 4 min. The GC oven temperature started at 120  $^{\circ}\text{C}$ , was held for 1 min, ramped at 20  $^{\circ}\text{C min}^{-1}$  to 160  $^{\circ}\text{C}$ , then ramped at 4  $^{\circ}\text{C min}^{-1}$  to 200  $^{\circ}\text{C}$ , then at 25  $^{\circ}\text{C min}^{-1}$  to 325  $^{\circ}\text{C}$ , and held 4 min to give a total run time of 22 min. The MS was run in electron capture negative chemical ionization (ECNI) mode using selective ion monitoring (SIM). Samples were quantified from a 10-point calibration curve based on the ratios of the target peak areas to the corresponding surrogate peak area. A list of all target BFRs and isotopically labelled PCB surrogate and their MS parameters, including chromatographic retention times, quantification ions, and confirmation ions are listed in Table S2.

**Table S2. GC-MS retention times (RT), quantification, and confirmation ions for BFRs in ECNI.**

SIM Window	Compound	RT (min)	Quantification Ion		Confirmation Ions	
			Q1	Q2	Q3	Q4
1	BDE-17	6.81	79.0	81.0	326.9	
	BDE-28	7.36	79.0	81.0	326.9	
<b>2</b>	<b>13C-PCB-178</b>	<b>8.87</b>	<b>405.7</b>	<b>407.6</b>	<b>409.6</b>	
3	BDE-71	10.46	79.0	81.0	160.8	324.9
	BDE-47	10.96	79.0	81.0	160.8	324.9
	BDE-66	11.59	79.0	81.0	160.8	324.9
4	BDE-100	13.72	79.0	81.0	160.8	402.8
	BDE-99	14.24	79.0	81.0	160.8	402.8
	BDE-85	14.82	79.0	81.0	160.8	402.8
5	BDE-154	15.10	79.0	81.0	328.6	563.6
6	BDE-153	15.48	79.0	81.0	328.6	564.6
7	BDE-138	15.88	79.0	81.0	403.5	563.6
8	BDE-183	16.30	79.0	81.0	561.6	
	BTBPE	16.53	79.0	81.0	328.6	
9	BDE-209	19.00	488.4	79.0	81.0	486.5

**Section 3. Recommendations for the analysis of BDE-209.**

This section contains additional comments and recommendations that may be of use to chromatographers wishing to analyze BDE-209. First, we found that the single most important factor for improving the response of BDE-209 was the type of liner. Peak heights of most target BFRs almost doubled with the use of a drilled-uniliner for direct injections over the standard single-tapered gooseneck liner used with the split/splitless injection port (Figure S3). For BDE-209, the peak height was close to four times as high. Additionally, we introduced a small portion of deactivated glass wool to the base of the liner. The purpose of the glass wool was to trap any flecks of septum that might have become dislodged from the inlet port during injection and to provide additional ‘hot’ surface area to facilitate the vaporization of the higher-molecular weight BFRs, for more efficient mass transfer to the head of the chromatographic column.

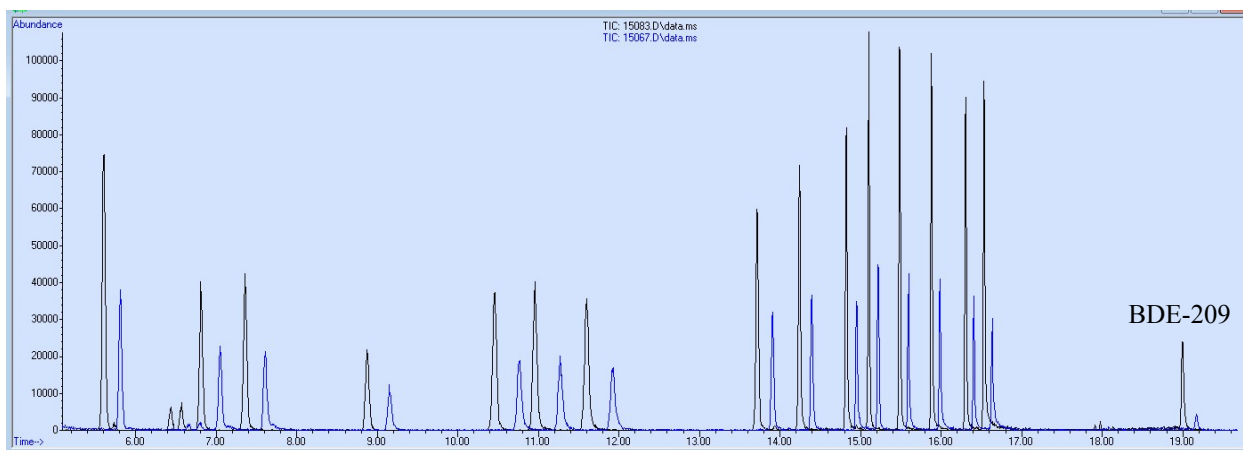


**Figure S3.** Comparison of total ion chromatograms for a BFR standard run under the same conditions using a) a standard single-tapered gooseneck splitless liner (blue) and b) a drilled uniliner for direct injections (black).

Optimization of a number of the parameters associated with mass selective detection improved the response for BDE-209. The ‘optimized’ tune parameters (100  $\mu$ A emission, 230 eV, and 250  $^{\circ}$ C source temperature) were selected by systematically varying one tune parameter at a time and comparing the average peak areas obtained for a BFR standard run in triplicate. We selected the combination of parameters that maximized the response for the target BFRs, particularly BDE-209. While the isotopically labelled surrogate compounds showed a greater response using the standard ECNI tune file (50  $\mu$ A emission, 230 eV, and 150  $^{\circ}$ C source temperature), all of the target BFRs had greater responses with the optimized tune file. Similar improvements in PBDE responses have been observed previously for non-standard tune parameters.<sup>9</sup>

Finally, we noticed the peak shapes of the BFRs were significantly worse when a 5-m deactivated guard column was installed at the head of the column, with very noticeable peak tailing for the tetra- to hexa-BDEs. While removal of the guard column meant routine maintenance, such as clipping of the main column and replacement of the liner, was required more frequently, the improvements in peak shape outweighed the annoyance of additional instrument down time. For chromatographers experiencing significant tailing with their PBDE analyses, we recommend removing the guard column where the samples are clean enough to run without one.

#### **Section 4. Details of the quality control measures.**

##### *Monitoring the chromatographic analysis*

A 10 pg  $\mu\text{L}^{-1}$  check standard containing all the target and surrogate BFRs was run after each set of six samples to monitor instrument performance and to test the stability and reliability of the calibration curve. The deviation between the known concentrations in the check standard and the concentrations measured using the calibration curve were calculated and when the deviation exceeded 30%, maintenance was performed and/or the calibration standards were run again to establish a new calibration curve.

##### *Extraction method recoveries*

Recovery analyses were performed by spiking a mixture of target BFRs of known concentration (10  $\mu\text{L}$  of 2000 pg  $\mu\text{L}^{-1}$ ) into the pre-cleaned PUF or pre-baked QFF matrices prior to extraction. Following the extraction, clean-up, and solvent reduction steps, the concentrated extracts were spiked with 15  $\mu\text{L}$  of a 2000 pg  $\mu\text{L}^{-1}$  standard containing the isotopically labelled  $^{13}\text{C}_{12}$ -PCB-178 solution prior to analysis using GC-MS. A ‘full recovery’ standard containing 270  $\mu\text{L}$  of ethyl acetate was prepared in series with each set of extracted matrices and spiked with the same mixtures of target BFRs and isotopically labelled PCB surrogate that were used for real samples. The method recoveries were calculated as a percentage of the full recovery standard, which accounted for any errors or irregularities that may have unwillingly occurred during the spiking procedure (i.e., if the syringe was not dispensing the correct volume or the actual concentrations in the spiking solution were different to the expected concentrations).

For the high-volume air sampling (HVS) media, the recoveries of the 14 target BFRs ranged from 70 to 93% (mean of 84%) and 70 to 88% (mean of 81%) in the QFF and PUF, respectively (Figure S4), with an average %RSD of 9% for triplicate measurements with QFF and 11% for four replicates with PUF. For the flow-through air sampling (FTS) PUF, BFR recoveries ranged from 50 to 107% (mean of 62%), with an average %RSD of 34% ( $n = 3$ ). The poorer recoveries observed for the FTS PUF were perhaps not surprising for a number of reasons: a) each sample was extracted in two parts and recombined, introducing greater opportunities for error and analyte loss (e.g., via volatilization) and b) there was an obvious chromatographic matrix effect observed between the full recovery standard (which did not contain any matrix components and exhibited poor peak shape) and the samples (containing matrix interferences, which greatly improved peak shape). Regardless, the use of the isotopically labelled surrogate spiked into every sample accounted for any losses or variability in the extraction efficiencies that may have occurred during the sample extraction, clean-up, and analysis.

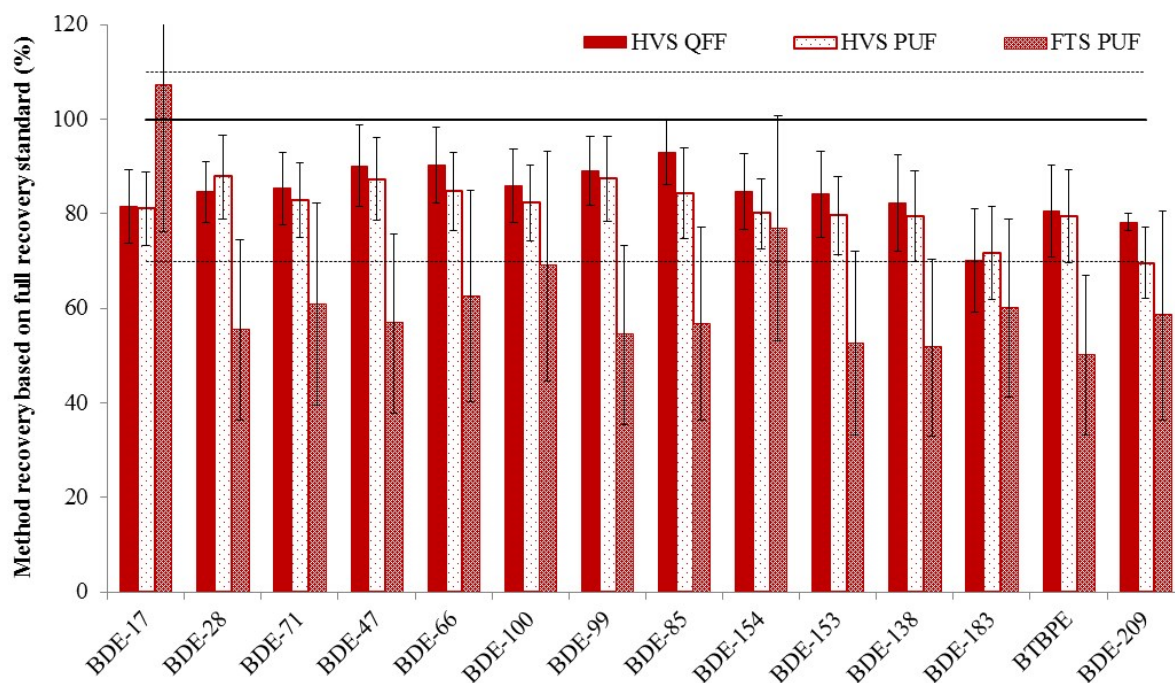


**Figure S4.** Extraction method recoveries for high-volume air sampling (HVS) QFF and PUF, and flow-through air sampling (FTS) PUF media based on a full recovery standard spiked with the same mass of target BFRs. Error bars represent  $\pm 1$  standard deviation ( $n = 3$  for HVS QFF and FTS PUF and  $n = 4$  for HVS PUF).

#### Sample-specific estimated detection limits

Sample-specific estimated detection limits (EDLs) were calculated using the approach described in EPA Method 8280A.<sup>10</sup> The EDL is an estimate of the concentration of a given target analyte required to produce a signal with a peak height of at least 2.5 times the background signal or ‘noise’ level. The estimates are sample-specific so need to be calculated for each different type of sampling media. Eq S3 was used to calculate the EDLs:

$$\text{EDL} = \frac{2.5 \times C_{s,s} \times H_{n,s} \times D}{V_i \times H_{s,s} \times \text{RF}} \quad (\text{eq S3})$$

where  $C_{s,s}$  is the concentration of the isotopically labelled surrogate ( $^{13}\text{C}_{12}$ -PCB-178) in the sample,  $H_{n,s}$  is the height of the noise in the sample for the quantitation ion (Q1) at the retention time of the target analyte if the analyte is absent from the sample or near the retention time of the target analyte if it is present in the sample,  $D$  is the dilution factor,  $V_i$  is the volume of air or water that was sampled ( $\text{m}^3$ ),  $H_{s,s}$  is the peak height of the quantitation ion of the isotopically labelled surrogate in the sample, and RF is the response factor, or the ratio of the height of the target analyte ( $H_{t,\text{std}}$ ) to that of the isotopically labelled surrogate ( $H_{s,\text{std}}$ ) in the lowest calibration standard in which the target analyte was still detected multiplied by the ratio of the concentration of the isotopically labelled surrogate ( $C_{s,\text{std}}$ ) to that of the target analyte ( $C_{t,\text{std}}$ ) in the same standard (eq S4). Thus, the calibration standard used to determine the RF varied depending on the specific target analyte and the lowest concentration at which it could be detected.

$$RF = \frac{H_{t, \text{std}}}{H_{s, \text{std}}} \times \frac{C_{s, \text{std}}}{C_{t, \text{std}}} \quad (\text{eq S4})$$

EDLs were calculated for five representative samples for the high-volume samples and three representative samples for the flow-through air sampling media, including the breakthrough PUF samples, and the averages of these were used in statistical analyses (Table S3). Higher EDLs result when the noise peaks are larger in the sample extracts. Thus, the higher EDLs for the flow-through air sampling PUF may reflect a greater level of matrix contamination.

**Table S3. Average EDLs for high-volume ( $n = 5$ ) and flow-through ( $n = 3$ ) air sampling media.**

Target BFR	High-volume air samples			Flow-through air samples	
	Breakthrough PUF (1x1" plug) (pg m <sup>-3</sup> )	Sample PUF (1x3" plug) (pg m <sup>-3</sup> )	Sample QFF (pg m <sup>-3</sup> )	Breakthrough PUF (1x1" plug) (pg m <sup>-3</sup> )	Sample PUF (4x1" plug) (pg m <sup>-3</sup> )
BDE-17	0.057	0.098	0.087	2.2	3.9
BDE-28	0.041	0.091	0.063	2.2	2.9
BDE-71	0.060	0.103	0.101	1.7	3.0
BDE-47	0.049	0.052	0.054	0.5	0.9
BDE-66	0.083	0.115	0.088	3.0	3.2
BDE-100	0.041	0.054	0.051	1.9	2.1
BDE-99	0.027	0.039	0.065	2.4	2.5
BDE-85	0.027	0.030	0.034	2.2	2.8
BDE-154	0.020	0.021	0.023	0.4	0.5
BDE-153	0.012	0.023	0.022	1.0	1.2
BDE-138	0.020	0.027	0.027	1.2	1.3
BDE-183	0.016	0.023	0.020	0.4	0.5
BTBPE	0.009	0.011	0.011	0.9	0.5
BDE-209	0.085	0.134	0.098	0.2	0.3

#### Laboratory blanks

A laboratory blank consisting of a 34-mL stainless steel extraction cell filled with pre-baked, acid-washed sand was extracted alongside each batch of ten samples to determine if there were residues of the target BFRs in the ambient laboratory or arising due to contamination of the analytical equipment.

BDE-47, -99, and -209 were detected in at least half of the laboratory blanks extracted alongside the QFF samples with average concentrations ranging from 64.9 to 332 fg  $\mu\text{L}^{-1}$ , which equated to less than 10% of the average target concentration measured in the sample QFFs. Similarly, BDE-47 and -99 were found in at least half of the laboratory blanks extracted alongside the PUF with average concentrations of 106 and 57.4 fg  $\mu\text{L}^{-1}$ , respectively, which equated to less than 2% of that in the PUF samples. No target BFRs were detected in the lab blanks run alongside the flow-through air samples, with the exception of BDE-209 on one occasion (21.8 pg  $\mu\text{L}^{-1}$ ).

Nevertheless, the contributions of residue target BFRs from the laboratory equipment were considered insignificant and a laboratory blank subtraction was deemed unnecessary.

*Field blanks*

Field blanks were collected periodically for each of the sampling media throughout the 60-d sampling period. Sampling media were introduced to the sampling cartridges in the same manner as samples for a timed 1-min exposure period while the samplers were turned off. Field blanks were stored and analyzed according to the procedures outlined for samples. Several BFRs were commonly detected in field blanks and we devised the following strategy to perform field blank subtractions: if the target BFRs were detected in at least half of the field blank samples, the average concentration in the field-blank samples where the target BFRs were detected was subtracted from the concentrations of the target BFRs in the actual samples (i.e., the concentrations listed in Table S4). If the target BFRs were detected in less than half of the field blank samples, no field blank subtraction was performed. In all cases, the field-blank subtracted concentrations of target BFRs were excluded if they were below the average estimated detection limit for the target BFR in the corresponding sampling media. All concentrations reported in the manuscript are field-blank subtracted.

**Table S4. Average concentrations of target BFRs that were measured in at least half of the high-volume and flow-through air sampler field blanks. ‘n.d.’ represents target BFRs that were not detected in any of the field blanks above their individual estimated detection limits and ‘-’ identifies target BFRs that were detected in less than half of the field blanks for which no field blank subtraction was performed.**

Target BFR	High-volume air samples			Flow-through air samples	
	PUF 1x1" plug (fg $\mu\text{L}^{-1}$ )	PUF 1x3" plug (fg $\mu\text{L}^{-1}$ )	QFF (fg $\mu\text{L}^{-1}$ )	PUF 1x1" plug (pg $\mu\text{L}^{-1}$ )	PUF 4x1" plug (pg $\mu\text{L}^{-1}$ )
BDE-17	n.d.	n.d.	n.d.	-	-
BDE-28	-	-	n.d.	-	-
BDE-71	n.d.	n.d.	n.d.	n.d.	n.d.
BDE-47	140	561	-	76.1	304
BDE-66	n.d.	n.d.	n.d.	n.d.	n.d.
BDE-100	-	-	n.d.	10.6	42.4
BDE-99	79.2	317	-	26.5	106
BDE-85	-	-	n.d.	n.d.	n.d.
BDE-154	-	-	n.d.	5.7	22.8
BDE-153	43.5	174	-	5.0	19.9
BDE-138	-	-	n.d.	n.d.	n.d.
BDE-183	131	525	-	-	-
BTBPE	55.8	223	-	5.0	19.9
BDE-209	474	1900	1450	103	412

### *Breakthrough percentages*

For both the HVS and FTS, a 1” breakthrough PUF was placed at the outlet of the sample cartridge to determine whether target BFRs were being lost from the preceding sample PUF plug(s). The breakthrough percentages of target BFRs were calculated using eq S5.

$$\text{Breakthrough \%} = \frac{[\text{breakthrough PUF}]}{[\text{breakthrough PUF}] + [\text{sample PUF}]} \cdot 100 \quad (\text{eq S5})$$

where [breakthrough PUF] is the concentration of the target BFR in the breakthrough PUF plug and [sample PUF] is the concentration of the target BFR in the corresponding sample PUF plugs (1x 3” PUF plug for HVS and 4x 1” PUF plugs for FTS).

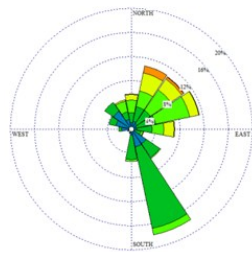
Breakthrough of target BFRs into the 1” PUF plug at the base of the HVS air sampling cartridge was minimal during the 48-h sampling period. BDE-47 was detected in only one of the breakthrough plugs with a concentration of 0.06 pg m<sup>-3</sup>, which equated to 2% of the total mass of BDE-47 trapped in the PUF cartridge for that sample. Additionally, BDE-209 was detected in the breakthrough plugs on three occasions with concentrations ranging from 0.13 to 0.14 pg m<sup>-3</sup>. On two of those occasions BDE-209 was not detected in the 3”-PUF sample plug and on the third occasion, breakthrough was less than 4%. BDE-209 is typically associated with particulate matter and one would not expect to detect it in the PUF (which samples gas-phase BFRs), nor to observe breakthrough. BDE-209 residues were originally quantified in all of the breakthrough PUF plugs; however, after the field blank subtraction, only three of those observations remained above the EDL. The average field-blank concentration for BDE-209 in the breakthrough PUF was 474.2 pg m<sup>-3</sup> (range 334.6-703.8 pg m<sup>-3</sup>). If the maximum BDE-209 field blank concentration (703.8 pg m<sup>-3</sup>) had been subtracted from the concentrations of BDE-209 measured in the breakthrough PUF instead of the average (474.2 pg m<sup>-3</sup>), all the reported concentrations would have fallen below the EDL (i.e., BDE-209 classified as ‘not detected’, thus 0% breakthrough). Therefore, it seems fair to conclude that the presence of BDE-209 in the breakthrough PUF plugs were artefacts associated with the field blank subtraction and that breakthrough of target BFRs was negligible for the 48 h HVS. BDE-47 was the most frequently detected BFR in the FTS breakthrough PUF plug and breakthrough percentages >20% were more frequently observed for BDE-47 and -99, and in some cases BDE-28, -154, and -209 at the Toolik Lake and Imnavait Creek sites during the first sampling period and the Oksrukuyik Creek site during the final sampling period. Overall, the average breakthrough percentages were generally higher for the FTS (~20%) than the HVS; although 60% of the BDE measurements did not show any breakthrough. This is not surprising given the potential for the FTS to act as both a wind-driven active sampler and a diffusion-based passive sampler (that could account for the presence of BFRs in the breakthrough PUF plug, which may have accumulated during calm periods).

**Table S5. Summary of average 24-hour meteorological data during the 60-day sampling period at Toolik Field Station.**

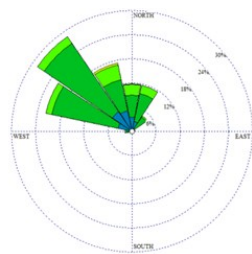
#	Julian day	Date	Air temperature (°C)	Lake water temperature (°C)	Relative humidity (%)	Wind speed (m s <sup>-1</sup> )	Wind direction*	Rainfall (mm)	Atmospheric pressure (mbar)
1	187	2013-07-06	12.2	8.8	58.8	2.8	ENE	0.0	927.5
2	188	2013-07-07	11.8	9.3	70.3	3.7	NNE	0.0	922.4
3	189	2013-07-08	3.8	10.5	99.4	2.7	NW	0.2	923.9
4	190	2013-07-09	5.9	10.4	93.8	2.7	NNE	0.0	931.7
5	191	2013-07-10	7.5	10.3	91.4	2.5	N	0.0	936.7
6	192	2013-07-11	10.2	10.5	70.9	3.2	NE	0.0	937.4
7	193	2013-07-12	12.7	10.9	60.6	2.2	NNW	0.0	935.5
8	194	2013-07-13	16.3	11.0	55.7	2.4	NNE	0.0	934.2
9	195	2013-07-14	18.0	11.2	50.7	3.3	NE	0.0	935.1
10	196	2013-07-15	15.6	11.9	71.1	3.7	WNW	0.0	934.6
11	197	2013-07-16	13.6	12.6	81.6	1.6	NW	0.4	932.0
12	198	2013-07-17	9.6	13.0	90.7	2.7	NW	0.1	933.6
13	199	2013-07-18	12.0	12.9	78.8	1.9	NNE	0.1	933.9
14	200	2013-07-19	10.4	13.6	93.0	3.0	N	0.9	932.6
15	201	2013-07-20	9.2	13.6	90.1	2.7	NNE	0.2	933.1
16	202	2013-07-21	13.2	12.9	67.3	1.3	SSW	0.0	934.4
17	203	2013-07-22	14.1	12.8	66.6	3.8	SSW	0.0	932.6
18	204	2013-07-23	9.2	12.9	91.7	2.2	NNW	0.2	932.7
19	205	2013-07-24	5.6	13.1	85.6	3.4	WNW	0.0	933.9
20	206	2013-07-25	8.3	12.9	74.4	3.1	NW	0.0	934.5
21	207	2013-07-26	10.7	12.7	81.3	2.1	W	0.4	936.5
22	208	2013-07-27	12.4	12.5	89.3	4.0	SW	0.2	938.4
23	209	2013-07-28	15.7	12.5	69.8	3.2	W	0.0	932.0
24	210	2013-07-29	10.9	12.7	85.1	3.6	W	0.1	936.1
25	211	2013-07-30	12.7	12.6	82.8	2.4	WNW	0.1	936.0
26	212	2013-07-31	10.3	12.9	90.0	2.6	WNW	0.0	935.4
27	213	2013-08-01	15.0	12.8	64.8	2.9	S	0.0	930.1
28	214	2013-08-02	16.2	12.9	67.6	3.6	S	0.0	925.6
29	215	2013-08-03	15.3	13.2	67.1	3.1	SSE	0.0	921.0
30	216	2013-08-04	13.5	13.2	60.8	6.2	SSW	0.0	924.0
31	217	2013-08-05	11.0	13.1	82.4	4.6	E	0.1	930.3

#	Julian day	Date	Air temperature (°C)	Lake water temperature (°C)	Relative humidity (%)	Wind speed (m s <sup>-1</sup> )	Wind direction*	Rainfall (mm)	Atmospheric pressure (mbar)
32	218	2013-08-06	14.8	12.9	58.7	3.5	161.8 SSE	0.0	931.7
33	219	2013-08-07	18.0	13.0	56.6	3.4	169.7 S	0.1	924.9
34	220	2013-08-08	15.0	13.3	59.0	5.2	187.2 S	0.0	921.5
35	221	2013-08-09	14.3	13.4	67.0	3.6	172.7 S	0.0	921.3
36	222	2013-08-10	11.8	13.4	67.8	2.7	189.5 S	0.1	927.7
37	223	2013-08-11	13.0	13.5	66.3	3.3	84.5 E	0.0	934.2
38	224	2013-08-12	11.1	13.5	87.6	1.6	35.5 NE	0.2	934.7
39	225	2013-08-13	11.4	13.6	86.4	2.4	43.7 NE	0.0	931.5
40	226	2013-08-14	5.1	13.5	100.0	2.2	334.5 NNW	0.6	928.6
41	227	2013-08-15	6.7	13.2	94.0	2.2	34.0 NE	0.0	927.2
42	228	2013-08-16	6.6	13.0	97.9	1.8	359.4 N	0.1	923.3
43	229	2013-08-17	5.2	12.7	99.0	2.5	353.5 N	0.2	922.4
44	230	2013-08-18	3.6	12.4	97.6	3.8	28.2 NNE	0.0	920.7
45	231	2013-08-19	0.4	11.7	98.4	3.8	27.6 NNE	0.2	922.5
46	232	2013-08-20	-4.7	10.8	94.9	3.6	43.6 NE	0.1	926.3
47	233	2013-08-21	0.6	10.3	73.3	1.6	176.3 S	0.0	923.2
48	234	2013-08-22	2.5	10.1	72.1	1.9	28.4 NNE	0.0	921.3
49	235	2013-08-23	-0.5	9.8	96.9	1.5	354.9 N	0.1	925.2
50	236	2013-08-24	0.1	9.5	84.5	1.7	22.8 NNE	0.0	930.3
51	237	2013-08-25	-1.4	9.2	84.2	2.3	78.1 ENE	0.0	929.7
52	238	2013-08-26	4.2	8.9	63.2	2.5	150.3 SSE	0.0	926.8
53	239	2013-08-27	7.6	8.7	45.3	3.6	185.3 S	0.0	921.1
54	240	2013-08-28	5.4	8.4	71.0	4.5	145.4 SE	0.5	920.6
55	241	2013-08-29	3.0	8.4	93.9	2.7	312.1 NW	0.0	924.3
56	242	2013-08-30	-2.4	8.1	89.5	3.7	217.0 SW	0.2	926.8
57	243	2013-08-31	-4.6	7.5	73.9	4.1	146.4 SSE	0.0	930.1
58	244	2013-09-01	-0.5	7.2	64.9	2.8	92.2 E	0.0	925.6
59	245	2013-09-02	5.8	7.0	54.3	4.0	99.9 E	0.3	916.5
60	246	2013-09-03	6.1	7.1	84.7	4.2	288.5 WNW	0.0	910.6

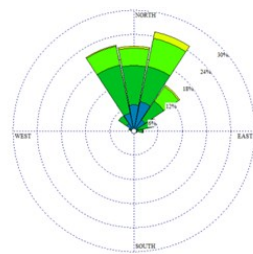
\* Average wind directions were calculated using the vector averaging method,<sup>11</sup> which weights the directions according to the concurrent wind speed observation.



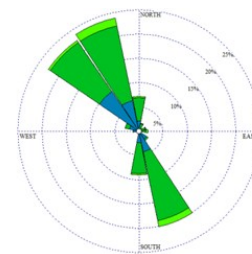
**Julian day 187-188**  
Calms: 5.28%



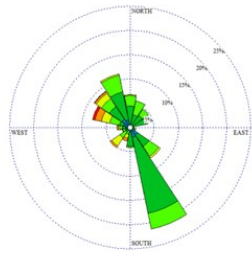
**Julian day 189-190**  
Calms: 0.83%



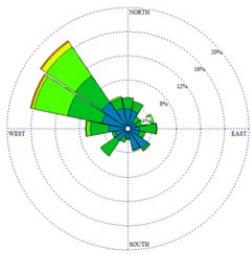
**Julian day 191-192**  
Calms: 2.21%



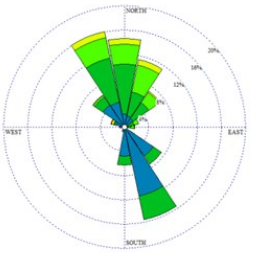
**Julian day 193-194**  
Calms: 3.59%



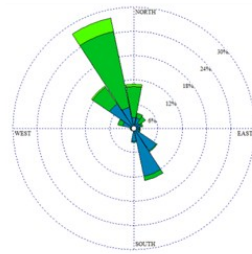
**Julian day 195-196**  
Calms: 2.92%



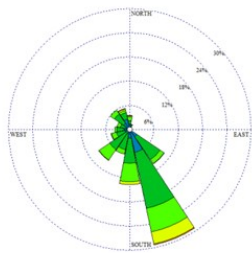
**Julian day 197-198**  
Calms: 8.37%



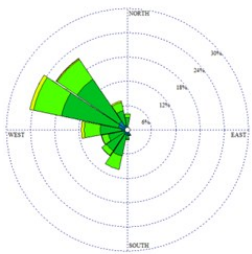
**Julian day 199-200**  
Calms: 6.19%



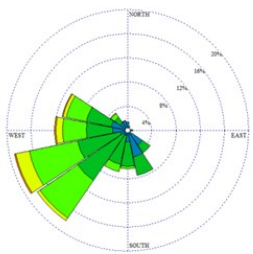
**Julian day 201-202**  
Calms: 4.37%



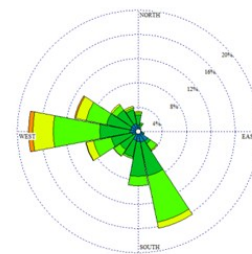
**Julian day 203-204**  
Calms: 2.49%



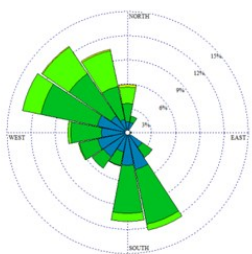
**Julian day 205-206**  
Calms: 1.37%



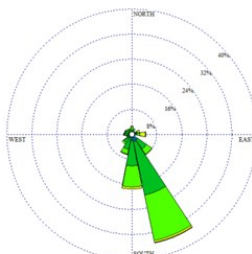
**Julian day 207-208**  
Calms: 5.12%



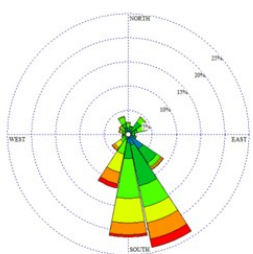
**Julian day 209-210**  
Calms: 6.33%



**Julian day 211-212**  
Calms: 3.62%



**Julian day 213-214**  
Calms: 3.31%



**Julian day 215-216**  
Calms: 3.38%

**Wind speed ( $\text{m s}^{-1}$ )**

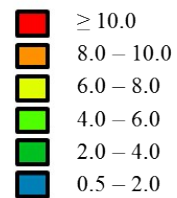


**Figure S5.** Wind roses showing the averaged 2-day wind frequency data during each high-volume air sampling period. Wind rose plots were prepared using WRPLOT View, version 7.0.0 (Lakes Environmental Software, 1998-2011).

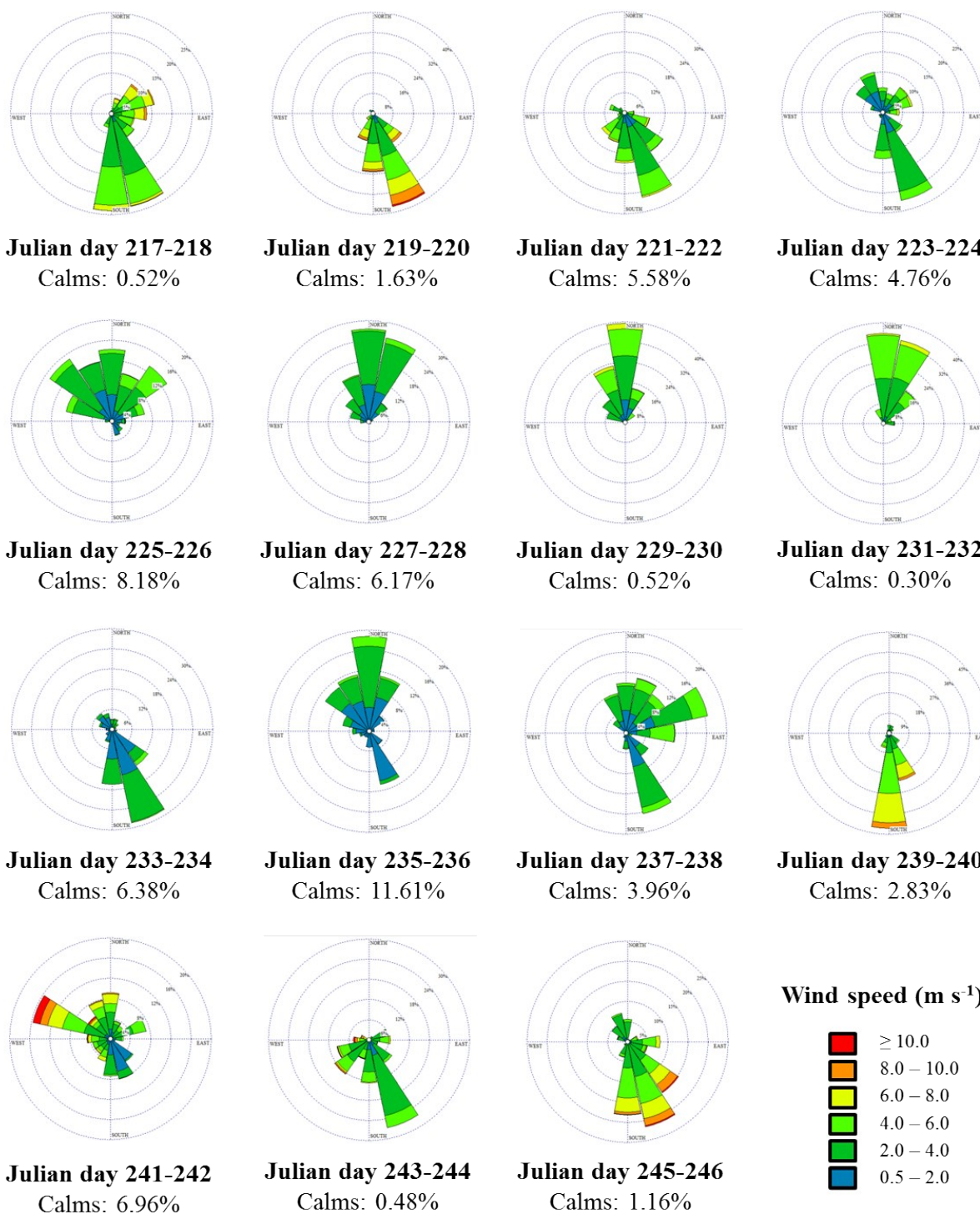


**Figure S5 continued.** Wind roses showing the averaged 2-day wind frequency data during each high-volume air sampling period. Wind rose plots were prepared using WRPLOT View, version 7.0.0 (Lakes Environmental Software, 1998-2011).

**Table S6. Gas-phase concentrations (pg m<sup>-3</sup>) of 14 target BFRs measured in high-volume air PUF samples at Toolik Lake, Alaska during a 60 d sampling period (6<sup>th</sup> July to 4<sup>th</sup> September 2013). For each BFR, the average, standard deviation (SD), minimum, and maximum concentrations over the season are listed in addition to the pooled 2 day sample concentration sums of the three predominant BDE congeners ( $\Sigma_3$ PBDEs: BDE-47, -99, and -100), all the PBDEs ( $\Sigma_{13}$ PBDEs), and all 14 BFRs, including BTBPE ( $\Sigma_{14}$ BFRs). Rows highlighted in grey represent samples whose data could not be reported due to problems that arose during sample extraction and analysis (e.g. sacrificed for method development or incorrect surrogate spiking). BFRs denoted with ‘n.d.’ were not detected in any of the 2-d PUF samples.**

#	Julian days	BDE-17	BDE-28	BDE-71	BDE-47	BDE-66	BDE-100	BDE-99	BDE-85	BDE-154	BDE-153	BDE-138	BDE-183	BTBPE	BDE-209	$\Sigma_3$ PBDEs	$\Sigma_{13}$ PBDEs	$\Sigma_{14}$ BFRs
1	187-188																	
2	189-190																	
3	191-192	0.37			7.09		0.49	0.71								8.28	8.65	8.65
4	193-194																	
5	195-196	0.41	0.66		9.74	0.35	1.23	2.78								13.8	15.2	15.2
6	197-198	0.18	0.36		4.04		0.48	0.88	0.05	0.04		0.04				5.40	6.08	6.08
7	199-200	0.23	0.43		4.20		0.41	0.76	0.06	0.06						5.37	6.15	6.15
8	201-202	0.26	0.61		4.62		0.51	0.77	0.06	0.06		0.04				5.89	6.92	6.92
9	203-204	0.21	0.33		4.63		0.57	1.23		0.04						6.43	7.01	7.01
10	205-206				0.80		0.11	0.06	0.04	0.41		0.04		0.14		0.97	1.60	1.60
11	207-208	0.14	0.20		2.50		0.37	0.79	0.05	0.05		0.032				3.66	4.13	4.13
12	209-210	0.26	0.31	0.27	4.52	0.20	0.74	1.87		0.07		0.04				7.14	8.28	8.28
13	211-212																	
14	213-214	0.33	0.35		6.26	0.23	1.19	3.37								10.8	11.7	11.7
15	215-216		0.28		3.36		0.61	1.47						1.11		5.44	6.84	6.84
16	217-218	0.20			2.81		0.44	1.02						0.13		4.27	4.60	4.60
17	219-220	0.26	0.25		3.59		0.77	2.09								6.46	6.96	6.96
18	221-222	0.21			2.14		0.45	1.00								3.59	3.79	3.79
19	223-224	0.19			2.02		0.48	1.15								3.65	3.84	3.84
20	225-226	0.12	0.17	0.27	1.26		0.30	0.54								2.11	2.67	2.67

#	Julian days	BDE-17	BDE-28	BDE-71	BDE-47	BDE-66	BDE-100	BDE-99	BDE-85	BDE-154	BDE-153	BDE-138	BDE-183	BTBPE	BDE-209	Σ <sub>3</sub> PBDEs	Σ <sub>13</sub> PBDEs	Σ <sub>14</sub> BFRs
21	227-228		0.58		0.60											0.60	1.19	1.19
22	229-230		0.61		0.28											0.28	0.89	0.89
23	231-232				0.07											0.07	0.07	0.07
24	233-234				0.35											0.35	0.35	0.35
25	235-236		0.14		0.14											0.14	0.28	0.28
26	237-238		0.12		0.60		0.06	0.08			0.18				0.62	0.74	1.67	1.67
27	239-240				0.51											0.51	0.51	0.51
28	241-242				0.33			0.04							3.32	0.37	3.69	3.69
29	243-244		0.12		0.28			0.08			0.69				2.58	0.36	3.76	3.76
30	245-246				0.55		0.07	0.05			0.026				0.68	0.67	1.38	1.38
	Minimum	0.12	0.12	0.27	0.07	0.20	0.06	0.04	0.04	0.04	0.03	0.03			0.13	0.07	0.07	0.07
	Maximum	0.41	0.66	0.27	9.74	0.35	1.23	3.37	0.06	0.41	0.69	0.04			3.32	13.8	15.2	15.2
	Average*	0.15	0.23	0.07	2.59	0.08	0.37	0.80	0.02	0.04	0.04	0.02	n.d.	n.d.	0.38	3.74	4.55	4.55
	SD*	0.1	0.2	0.06	2.5	0.07	0.4	0.9	0.02	0.08	0.1	0.01			0.8	3.6	3.8	3.8

\* Where target BFRs were not detected in a sample (left blank in the tabulated data above), they were replaced with a concentration of half the sample-specific EDL for calculations of seasonal averages and standard deviation ( $1/2$  EDLs are not shown in the tabulated data above).

**Table S7. Concentrations (pg m<sup>-3</sup>) of particle-bound BFRs measured in high-volume air QFF samples at Toolik Lake, Alaska during a 60-d sampling period (6<sup>th</sup> July to 4<sup>th</sup> September 2013). For each BFR, the average, standard deviation (SD), minimum, and maximum concentrations over the season are listed in addition to the pooled 2-d sample concentration sums of the three predominant BDE congeners ( $\Sigma_3$ PBDEs: BDE-47, -99, and -100), all the PBDEs ( $\Sigma_{13}$ PBDEs), and all 14 BFRs, including BTBPE ( $\Sigma_{14}$ BFRs). Rows highlighted in grey represent samples whose data could not be reported due to problems that arose during sample extraction and analysis (e.g. sacrificed for method development or incorrect surrogate spiking). BFRs denoted with ‘n.d.’ were not detected in any of the 2 d QFF samples.**

#	Julian days	BDE-17	BDE-28	BDE-71	BDE-47	BDE-66	BDE-100	BDE-99	BDE-85	BDE-154	BDE-153	BDE-138	BDE-183	BTBPE	BDE-209	$\Sigma_3$ PBDEs	$\Sigma_{13}$ PBDEs	$\Sigma_{14}$ BFRs
1	187-188																	
2	189-190																	
3	191-192																	
4	193-194				1.54		0.89	3.72		0.17	0.15					6.16	6.47	6.47
5	195-196				0.91		0.61	2.17	0.15	0.17	0.14			0.08		3.69	4.14	4.22
6	197-198				0.54		0.34	1.22	0.08	0.08	0.07			0.05		2.10	2.32	2.37
7	199-200				0.72		0.39	1.63		0.06					0.80	2.74	3.60	3.60
8	201-202				0.72		0.47	1.77		0.08	0.06					2.96	3.10	3.10
9	203-204				0.54		0.36	1.37		0.08	0.06					2.27	2.41	2.41
10	205-206				0.43		0.22	0.79			0.06		0.03			1.43	1.53	1.53
11	207-208				0.26		0.17	0.65	0.07	0.04	0.04			0.017		1.09	1.23	1.25
12	209-210				0.32		0.26	1.00		0.07	0.05			0.025		1.58	1.70	1.72
13	211-212				0.39		0.33	1.22	0.07	0.10	0.08					1.95	2.19	2.19
14	213-214				0.23		0.20	0.79		0.07	0.07			0.025		1.23	1.36	1.39
15	215-216				0.26		0.17	0.77	0.06	0.05	0.04					1.20	1.35	1.35
16	217-218				0.32		0.17	0.78		0.06			0.28	0.145		1.27	1.61	1.75
17	219-220				0.26		0.16	0.64		0.05	0.09		0.25	0.151		1.05	1.45	1.60
18	221-222				0.24		0.15	0.63		0.05	0.06		0.26	0.128	2.05	1.01	3.44	3.56
19	223-224				0.17		0.15	0.60	0.08	0.08	0.07		0.03	0.037	0.57	0.92	1.75	1.79

20	225-226				0.17		0.12	0.54	0.06	0.04	0.06					0.83	0.99	0.99
#	Julian days	BDE-17	BDE-28	BDE-71	BDE-47	BDE-66	BDE-100	BDE-99	BDE-85	BDE-154	BDE-153	BDE-138	BDE-183	BTBPE	BDE-209	Σ <sub>3</sub> PBDEs	Σ <sub>13</sub> PBDEs	Σ <sub>14</sub> BFRs
21	227-228				0.23		0.15	0.47		0.05	0.06		0.03	0.036	0.17	0.85	1.16	1.19
22	229-230		0.08		0.20			0.21					0.04		0.19	0.41	0.72	0.72
23	231-232				0.18			0.16					0.03		0.38	0.35	0.76	0.76
24	233-234				0.24		0.10	0.30					0.05			0.64	0.69	0.69
25	235-236		0.08		0.17		0.06	0.16							1.75	0.39	2.22	2.22
26	237-238				0.17			0.22							6.64♦	0.39	7.03	7.03
27	239-240				0.19		0.09	0.29							2.33	0.57	2.91	2.91
28	241-242				0.09			0.16								0.25	0.25	0.25
29	243-244				0.12			0.07							0.61	0.19	0.80	0.80
30	245-246				0.09			0.19							0.52	0.28	0.80	0.80
	Minimum		0.08		0.09		0.06	0.07	0.06	0.04	0.04		0.03	0.02	0.17	0.19	0.25	0.25
	Maximum		0.08		1.54		0.89	3.72	0.15	0.17	0.15		0.28	0.15	6.64	6.16	7.03	7.03
	Average*	n.d.	0.04	n.d.	0.36	n.d.	0.21	0.83	0.03	0.05	0.05	n.d.	0.04	0.03	0.62	1.40	2.15	2.17
	SD*		0.01		0.3		0.2	0.8	0.03	0.04	0.04		0.08	0.04	1.4	1.3	1.7	1.7

\* Where target BFRs were not detected in a sample (left blank in the tabulated data above), they were replaced with a concentration of half the sample-specific EDL for calculations of seasonal averages and standard deviation ( $1/2$  EDLs are not shown in the tabulated data above).

♦ Concentration measured in the sample was outside the upper limit of the calibration curve and should be considered semi-quantitative.

**Table S8.** Total concentrations (pg m<sup>-3</sup>) of target BFRs (gas-phase + particle-bound) measured in high-volume air samples at Toolik Lake, Alaska during a 60-d sampling period (6<sup>th</sup> July to 4<sup>th</sup> September 2013). For each BFR, the average, standard deviation (SD), minimum, and maximum concentrations over the season are listed in addition to the pooled 2-d sample concentration sums of the three predominant BDE congeners ( $\Sigma_3$ PBDEs: BDE-47, -99, and -100), all the PBDEs ( $\Sigma_{13}$ PBDEs), and all 14 BFRs, including BTBPE ( $\Sigma_{14}$ BFRs). Rows highlighted in grey represent the samples that were sacrificed for method development.

#	Julian days	BDE-17	BDE-28	BDE-71	BDE-47	BDE-66	BDE-100	BDE-99	BDE-85	BDE-154	BDE-153	BDE-138	BDE-183	BTBPE	BDE-209	$\Sigma_3$ PBDEs	$\Sigma_{13}$ PBDEs	$\Sigma_{14}$ BFRs
1	187-188																	
2	189-190																	
3	191-192	0.37			7.09		0.49	0.71								8.3	8.6	8.6
4	193-194				1.54		0.89	3.72		0.17	0.15					6.2	6.5	6.5
5	195-196	0.41	0.66		10.65	0.35	1.85	4.94	0.15	0.17	0.14			0.08		17.4	19.3	19.4
6	197-198	0.18	0.36		4.57		0.82	2.10	0.13	0.12	0.07	0.04		0.05		7.5	8.4	8.5
7	199-200	0.23	0.43		4.92		0.80	2.39	0.06	0.13					0.80	8.1	9.7	9.7
8	201-202	0.26	0.61		5.34		0.98	2.54	0.06	0.14	0.06	0.04				8.9	10.0	10.0
9	203-204	0.21	0.33		5.17		0.93	2.60		0.12	0.06					8.7	9.4	9.4
10	205-206				1.23		0.33	0.85	0.04	0.41	0.06	0.04	0.03		0.14	2.4	3.1	3.1
11	207-208	0.14	0.20		2.76		0.54	1.44	0.12	0.09	0.04	0.03		0.02		4.7	5.4	5.4
12	209-210	0.26	0.31	0.27	4.84	0.20	1.00	2.87		0.13	0.05	0.04		0.02		8.7	10.0	10.0
13	211-212				0.39		0.33	1.22	0.07	0.10	0.08					1.9	2.2	2.2
14	213-214	0.33	0.35		6.49	0.23	1.40	4.17		0.07	0.07			0.02		12.1	13.1	13.1
15	215-216		0.28		3.62		0.79	2.25	0.06	0.05	0.04				1.11	6.6	8.2	8.2
16	217-218	0.20			3.13		0.62	1.79		0.06			0.28	0.15	0.13	5.5	6.2	6.4
17	219-220	0.26	0.25		3.85		0.93	2.73		0.05	0.09		0.25	0.15		7.5	8.4	8.6
18	221-222	0.21			2.38		0.59	1.63		0.05	0.06		0.26	0.13	2.05	4.6	7.2	7.4
19	223-224	0.19			2.19		0.63	1.75	0.08	0.08	0.07		0.03	0.04	0.57	4.6	5.6	5.6
20	225-226	0.12	0.17	0.27	1.43		0.42	1.08	0.06	0.04	0.06					2.9	3.7	3.7

21	227-228	0.58	0.83	0.15	0.47	0.05	0.06	0.03	0.04	0.17	1.5	2.3	2.4					
#	Julian days	BDE-17	BDE-28	BDE-71	BDE-47	BDE-66	BDE-100	BDE-99	BDE-85	BDE-154	BDE-153	BDE-138	BDE-183	BTBPE	BDE-209	$\Sigma_3$ PBDEs	$\Sigma_{13}$ PBDEs	$\Sigma_{14}$ BFRs
22	229-230	0.69			0.48			0.21					0.04		0.19	0.7	1.6	1.6
23	231-232				0.26			0.16					0.03		0.38	0.4	0.8	0.8
24	233-234				0.59		0.10	0.30					0.05			1.0	1.0	1.0
25	235-236	0.22			0.31		0.06	0.16							1.75	0.5	2.5	2.5
26	237-238	0.12			0.77		0.06	0.30		0.18					7.26 <sup>♦</sup>	1.1	8.7	8.7
27	239-240				0.69		0.09	0.29							2.33	1.1	3.4	3.4
28	241-242				0.42			0.20							3.32	0.6	3.9	3.9
29	243-244	0.12			0.40			0.15		0.69					3.19	0.5	4.6	4.6
30	245-246				0.64		0.07	0.24		0.03					1.20	0.9	2.2	2.2
	Minimum	0.12	0.12	0.27	0.26	0.20	0.06	0.15	0.04	0.04	0.03	0.03	0.03	0.02	0.13	0.4	0.8	0.8
	Maximum	0.41	0.69	0.27	10.65	0.35	1.85	4.94	0.15	0.41	0.69	0.04	0.28	0.15	7.26	17.4	19.3	19.4
	Average*	0.18	0.25	0.11	2.75	0.12	0.54	1.55	0.05	0.08	0.09	0.03	0.05	0.03	0.95	4.8	6.3	6.3
	SD*	0.1	0.2	0.1	2.6	0.1	0.5	1.3	0.04	0.1	0.1	0.01	0.1	0.04	1.6	4.2	4.2	4.2

\* Where target BFRs were not detected in a sample (left blank in the tabulated data above), they were replaced with a concentration of half the sample-specific EDL for calculations of seasonal averages and standard deviation ( $1/2$  EDLs are not shown in the tabulated data above).

♦ Concentration measured in the sample was outside the upper limit of the calibration curve and should be considered semi-quantitative.

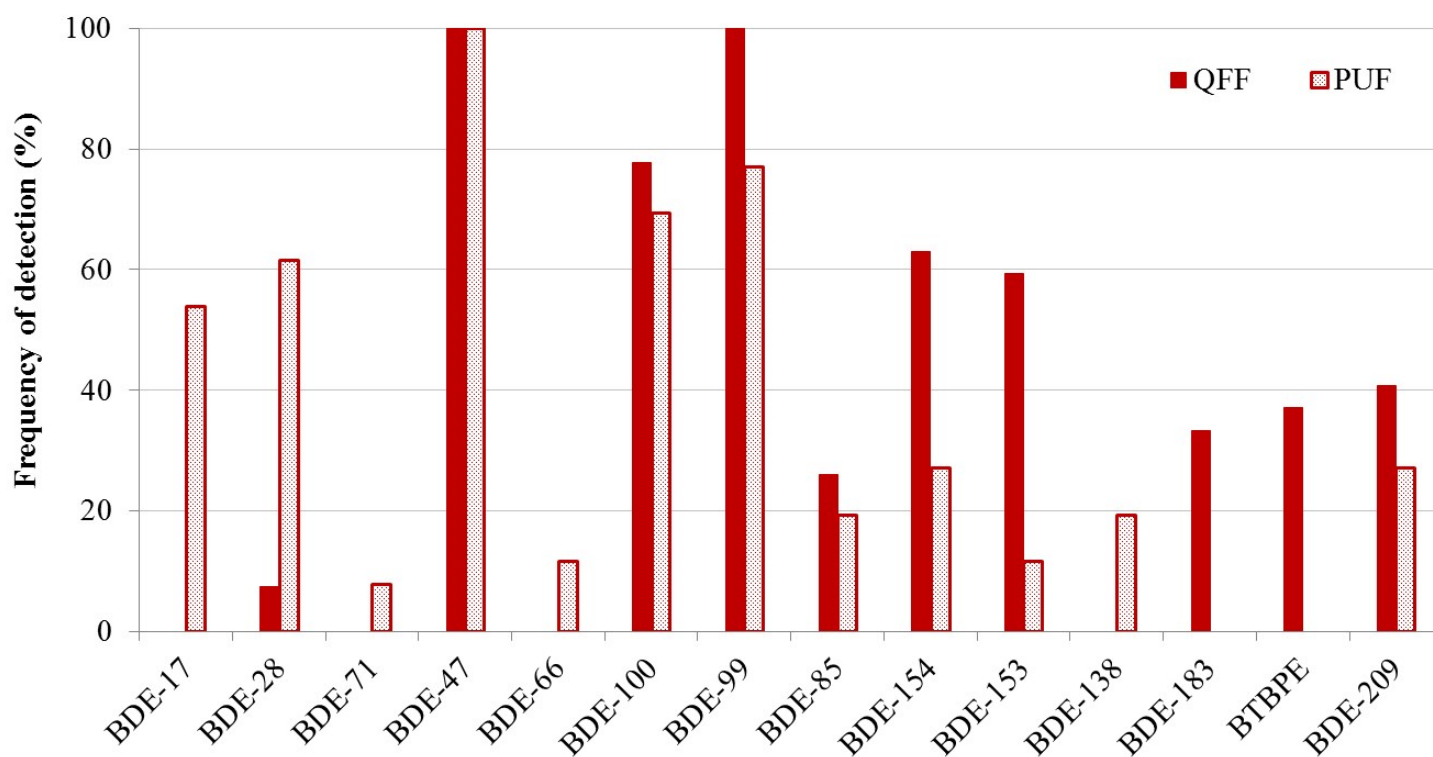


Figure S6. Frequency of detection for each of the target BFRs in high-volume air sampling QFF ( $n = 27$ ) and PUF ( $n = 26$ ).

**Table S9. Compilation of BFR concentrations in air reported at other Arctic sites.**

Location	Sampling period	Sampler	Concentrations (pg m <sup>-3</sup> )	BDE-47			BDE-99			BDE-100			BDE-209			BTBPE			Σ <sub>3</sub> PBDEs		
				Min	Max	Ave	Min	Max	Ave	Min	Max	Ave	Min	Max	Ave	Min	Max	Ave	Min	Max	Ave
<b>North America</b>																					
Toolik Lake, Alaska (This Study)	Summer 2013	HVS	Total	0.26	10.7	2.75	0.15	4.94	1.55	0.06	1.85	0.54	0.13	7.26	0.95	0.02	0.15	0.03	0.40	17.4	4.80
			Particle-bound	0.09	1.54	0.36	0.07	3.72	0.83	0.06	0.89	0.21	0.17	6.64	0.62	0.02	0.15	0.03	0.19	6.16	1.40
			Gas-phase	0.07	9.74	2.59	0.04	3.37	0.80	0.06	1.23	0.37	0.13	3.32	0.38				0.07	13.8	3.74
Barrow, Alaska	2004/2005	Passive <sup>12</sup>	Gas-phase																		5.00
	2005/2006	Passive <sup>13</sup>	Gas-phase												0.20	1.00	0.45				
St. Lawrence Island, Alaska	2005/2006	Passive <sup>13</sup>	Gas-phase												0.33	0.33	0.33				
Little Fox Lake, Yukon	2011-2014	FTS <sup>14</sup>	Total	0.21	6.83	1.20	0.18	7.06	0.96	0.04	1.27	0.19				0.02	0.22	0.08			
Alert, Canada	2002-2010	HVS <sup>15</sup>	Total	0.09	61.9	2.75	0.19	32.20	2.32	0.03	7.75	0.50	0.10	3.91	0.81*						
	2002-2004	HVS <sup>16</sup>	Total	0.21	18.0	2.50	0.19	22.0	2.40	0.03	2.50	0.45	0.09	9.80	1.60						
	2004/2005	Passive <sup>12</sup>	Gas-phase																		2.00
	2006/2007	FTS <sup>17</sup>	Total	0.25	12.0	2.70	0.06	5.30	0.65	0.20	31.0	3.20				0.16	1.90	0.85			
	2007/2008	FTS <sup>18</sup>	Total	0.03	7.20	1.57	0.02	5.90	1.22	0.02	1.30	0.31	0.04	0.33	0.19	0.01	0.80	0.30	0.07	14.4	3.10
	2007/2008	HVS <sup>18</sup>	Total	0.03	8.80	1.87	0.01	7.00	1.37	0.01	1.60	0.35	0.07	0.62	0.20	0.02	1.20	0.42	0.04	17.4	3.35
			Particle-bound	0.01	0.32	0.08	0.01	0.83	0.21	0.03	0.12	0.05	0.07	0.62	0.20	0.07	0.92	0.45	0.01	1.00	0.24
		Gas-phase	0.03	8.80	2.03	0.01	6.90	1.47	0.01	1.60	0.33	0.01	2.70	0.85	0.02	1.00	0.32	0.01	17.3	3.32	
<b>Europe</b>																					
Svalbard, Norway	Winter 2012/2013	HVS <sup>19</sup>	Particle-bound	0.23	4.10	0.82	0.07	6.80	0.69				0.12	6.80	1.30	0.01	0.09	0.04			
Zeppelin, Ny Ålesund, Norway	2006-2014	HVS <sup>15</sup>	Total	0.03	51.8	0.55	0.01	9.25	0.10	0.002	4.25	0.04	0.01	42.0	0.93						
	2004/2005	Passive <sup>12</sup>	Gas-phase																		5.30
	2005/2006	Passive <sup>13</sup>	Gas-phase													<0.2	5.20	1.75			
Nuuk, Greenland	2004/2005	HVS <sup>20</sup>	Total	0.08	1.40	0.46	0.05	1.20	0.36	0.01	0.22	0.08									

Location	Sampling period	Sampler	Concentrations (pg m <sup>-3</sup> )	BDE-47			BDE-99			BDE-100			BDE-209			BTBPE			Σ <sub>3</sub> PBDEs			
				Min	Max	Ave	Min	Max	Ave	Min	Max	Ave	Min	Max	Ave	Min	Max	Ave	Min	Max	Ave	
<b>Europe</b>																						
East Greenland Ocean	2009	HVS <sup>21</sup>	Total	0.06	0.95	0.36	0.01	0.51	0.13	0.002	0.12	0.03	0.05	0.07	0.06	0.003	0.08	0.02	0.07	1.58	0.52	
			Particle-bound	0.01	0.32	0.09	0.01	0.11	0.05	0.002	0.02	0.01	0.05	0.07	0.06	0.003	0.02	0.01	0.02	0.46	0.15	
			Gas-phase	0.05	0.82	0.30	0.04	0.46	0.11	0.01	0.11	0.03				0.04	0.06	0.05	0.05	1.39	0.41	
Storhofdi, Iceland	2008-2012	HVS <sup>15</sup>	Total	0.24	3.65	1.11	0.09	0.50	0.17													
Pallas, Finland	2013-2014	HVS <sup>15</sup>	Total	0.10	0.22	0.16	0.02	0.12	0.08	0.02	0.03	0.02										
<b>Arctic Ocean</b>																						
Arctic Ocean	2010	HVS <sup>22</sup>	Total	0.02	0.04	0.03	0.03	0.06	0.05	0.004	0.004	0.004	0.15	3.97	1.12	0.03	0.17	0.10	0.06	0.10	0.08	
			Particle-bound	0.01	0.01	0.01	0.01	0.01	0.01				0.15	3.43	0.90	0.03	0.03	0.03	0.01	0.02	0.02	
			Gas-phase	0.02	0.03	0.03	0.03	0.06	0.04	0.004	0.004	0.004	0.54	0.56	0.55	0.17	0.17	0.17	0.05	0.09	0.07	

\* BDE-209 was only analyzed from 2008 onwards.

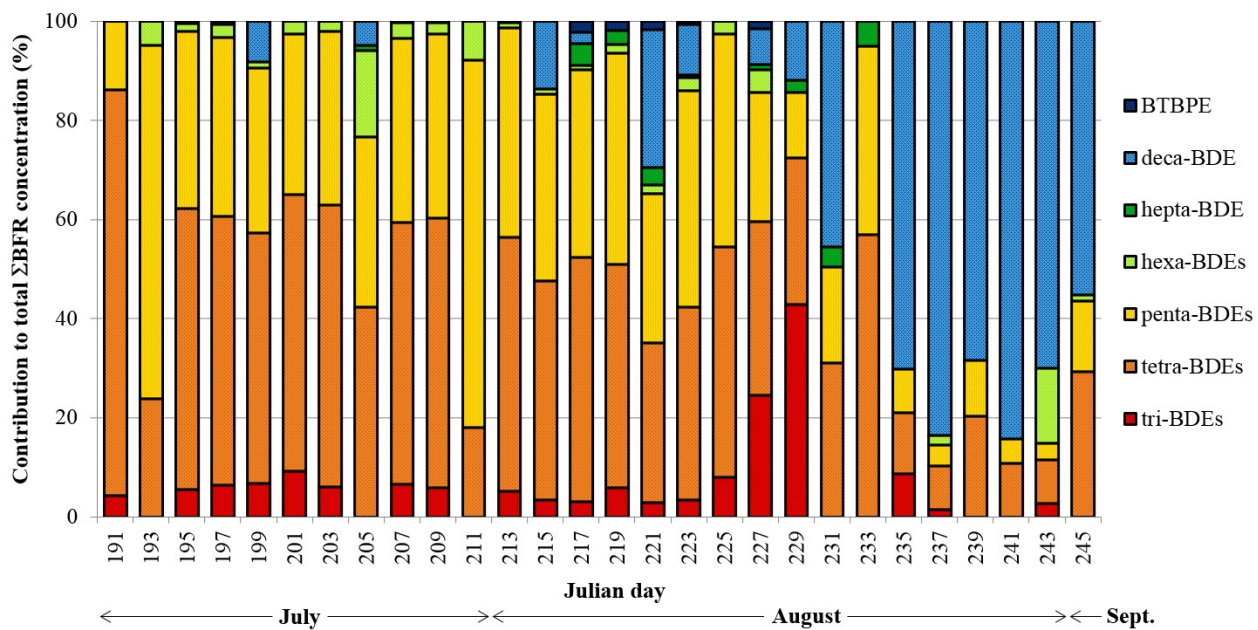
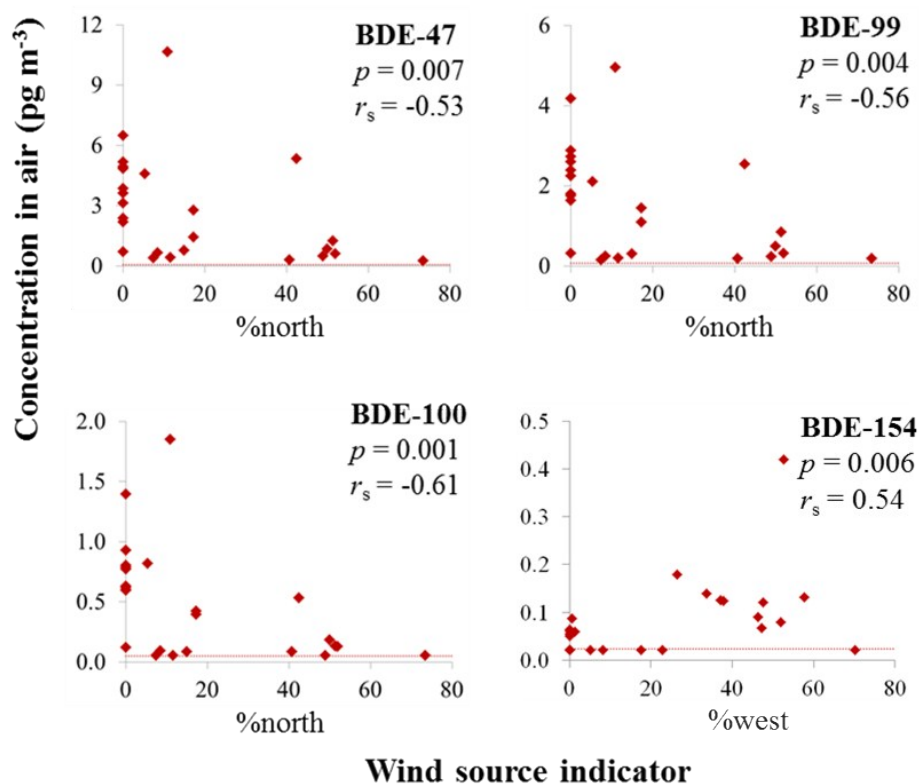
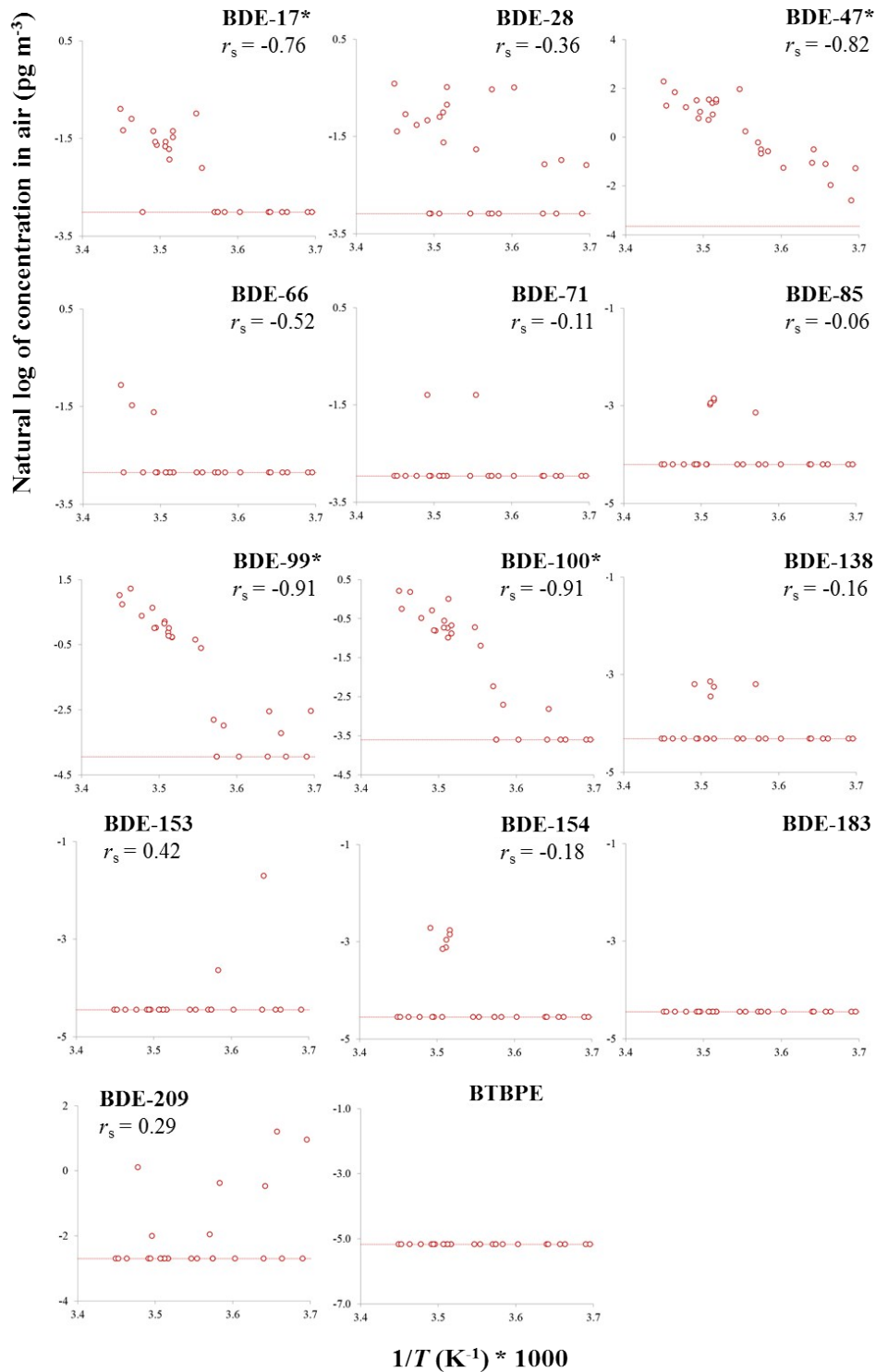


Figure S7. BFR profiles (combined gas- and atmospheric particle-bound phases) during the 60-d sampling period.



**Figure S8.** Regression plots with Spearman's rank ( $r_s$ , monotonic) correlation coefficients and  $p$ -values for source indicators versus the total concentrations in air (gas-phase and particle-bound) for BFRs. Only correlations that were significant ( $p < 0.05$ ) are displayed. BFRs that were not detected in a particular sample were replaced with concentration values representing half the sample-specific EDL for that target BFR (represented by the dotted horizontal line).



**Figure S9.** Regression plots with Spearman's rank ( $r_s$ , monotonic) correlation coefficients for average 48-h air temperatures versus the gas-phase concentrations in air for BFRs. BFRs that were detected in  $>30\%$  of the samples and whose correlations were significant ( $p < 0.05$ ) are denoted with an '\*'. BFRs that were not detected in a particular sample were replaced with concentration values representing half the sample-specific EDL for that target BFR (represented by the dotted horizontal line). Linear regressions are shown in solid black lines and were used to obtain a slope to gain information about possible sources.

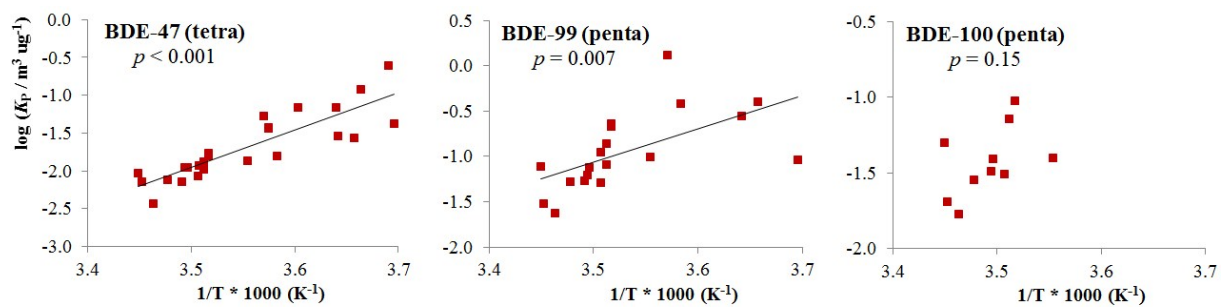


**Figure S10.** Correlations between  $\log K_p$  and inverse of temperature for selected BFRs, based on paired gas-phase and particle-bound concentrations in air.  $\log K_p$  values were calculated using a TSP of  $10 \mu\text{g m}^{-3}$ .

**Table S10.** Total concentrations ( $\text{pg m}^{-3}$ ) of target BFRs (gas-phase + particle-bound) measured in flow-through air samples at Toolik Lake, Alaska during three 18-d sampling periods (6<sup>th</sup> July to 29<sup>th</sup> August 2013). For each BFR, the minimum and maximum concentrations are listed in addition to the sums of the three predominant BDE congeners ( $\Sigma_3$ PBDEs: BDE-47, -99, and -100), all the PBDEs ( $\Sigma_{13}$ PBDEs), and all 14 BFRs, including BTBPE ( $\Sigma_{14}$ BFRs).

#	Location	BDE-17	BDE-28	BDE-71	BDE-47	BDE-66	BDE-100	BDE-99	BDE-85	BDE-154	BDE-153	BDE-138	BDE-183	BTBPE	BDE-209	$\Sigma_3$ PBDEs	$\Sigma_{13}$ PBDEs	$\Sigma_{14}$ BFRs
A	Toolik Lake				6.4			7.4	5.3	1.4		2.8	2.6	2.3	3.1	13.8	29.0	31.4
B	Toolik Lake				7.6				3.8	0.9		3.2	2.6	1.5		7.6	18.1	19.6
C	Toolik Lake												1.0				1.0	1.0
A	Imnavait		5.6		39.3			5.8					1.8			45.1	52.5	52.5
B	Imnavait				16.9			4.1							10.6	21.0	31.6	31.6
C	Imnavait																	
A	Oksrukuyik				26.5			8.2		0.8			2.6	0.8		34.7	38.1	39.0
B	Oksrukuyik				1.3										40.8	1.3	42.1	42.1
C	Oksrukuyik				19.5			5.5					1.9		31.5	24.9	58.4	58.4
	Minimum				1.3			4.1	3.8	0.8		2.8	1.0	0.8	3.1	1.3	1.0	1.0
	Maximum		5.6		39.3			8.2	5.3	1.4		3.2	2.6	2.3	40.8	45.1	58.6	58.6

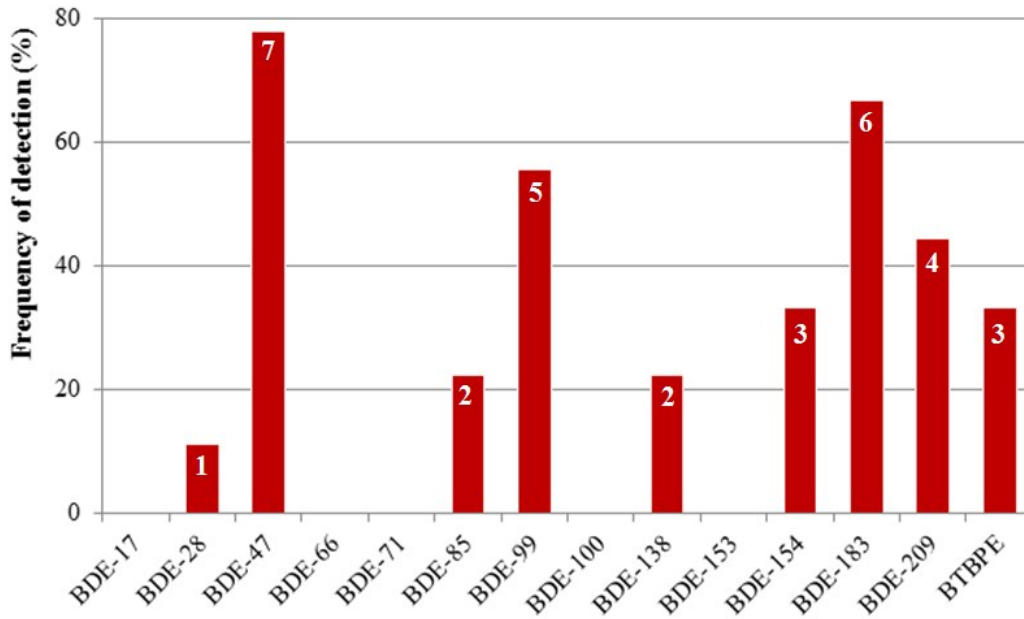


**Figure S11.** Frequency of detection for each of the target BFRs in flow-through air sampling PUF ( $n = 9$ ). The number of samples in which each BFR was actually detected is also shown within each bar.

## Section 5.       References

1. T. S. Geoghegan, K. J. Hageman and A. J. Hewitt, Testing flow-through air samplers for use in near-field vapour drift studies by measuring pyrimethanil in air after spraying. *Environ. Sci.-Process Impacts*, 2014, **16**, 422-432.
2. M. Shoeib and T. Harner, Characterization and comparison of three passive air samplers for persistent organic pollutants. *Environ. Sci. Technol.*, 2002, **36**, 4142-4151.
3. K. Pozo, T. Harner, M. Shoeib, R. Urrutia, R. Barra, O. Parra and S. Focardi, Passive-sampler derived air concentrations of persistent organic pollutants on a north-south transect in Chile. *Environ. Sci. Technol.*, 2004, **38**, 6529-6537.
4. R. Ghosh, K. J. Hageman and E. Bjorklund, Selective pressurized liquid extraction of three classes of halogenated contaminants in fish. *J. Chromatogr. A*, 2011, **1218**, 7242-7247.
5. Y. S. Su, H. Hung, K. A. Brice, K. Su, N. Alexandrou, P. Blanchard, E. Chan, E. Sverko and P. Fellin, Air concentrations of polybrominated diphenyl ethers (PBDEs) in 2002-2004 at a rural site in the Great Lakes. *Atmos. Environ.*, 2009, **43**, 6230-6237.
6. W. He, N. Qin, Q.-S. He, X.-Z. Kong, W.-X. Liu, Q.-M. Wang, C. Yang, Y.-J. Jiang, B. Yang, Z.-L. Bai, W.-J. Wu and F.-L. Xu, Atmospheric PBDEs at rural and urban sites in central China from 2010 to 2013: Residual levels, potential sources and human exposure. *Environ. Pollut.*, 2014, **192**, 232-243.
7. Z. Tang, Q. Huang, J. Cheng, Y. Yang, J. Yang, W. Guo, Z. Nie, N. Zeng and L. Jin, Polybrominated Diphenyl Ethers in Soils, Sediments, and Human Hair in a Plastic Waste Recycling Area: A Neglected Heavily Polluted Area. *Environ. Sci. Technol.*, 2014, **48**, 1508-1516.
8. B. Subedi, L. Aguilar, E. M. Robinson, K. J. Hageman, E. Björklund, R. J. Sheesley and S. Usenko, Selective pressurised liquid extraction as a sample-preparation technique for organic pollutants and contaminants of emerging concern. *TRAC-Trend Anal Chem*, 2015, **68**, 119-132.
9. L. K. Ackerman, G. R. Wilson and S. L. Simonich, Quantitative analysis of 39 polybrominated diphenyl ethers by isotope dilution GC/low-resolution MS. *Anal. Chem.*, 2005, **77**, 1979-1987.
10. EPA Method 8280A: The Analysis of Polychlorinated Dibenzo-p-Dioxins and Polychlorinated Dibenzofurans by High Resolution Gas Chromatography/Low Resolution Mass Spectrometry (HRGC/LRMS), [http://www.well-labs.com/docs/epa%208280a\\_dec1996.pdf](http://www.well-labs.com/docs/epa%208280a_dec1996.pdf), (accessed 28 October, 2014).
11. M. Haysom, Vector manipulation. What is the average of northeast and northwest? *Australian Senior Mathematics Journal*, 2001, **15**, 4-8.
12. K. Pozo, T. Harner, F. Wania, D. Muir, K. C. Jones and L. Barrie, Toward a global network for persistent organic pollutants in air: Results from the GAPS study. *Environ. Sci. Technol.*, 2006, **40**, 4867-4873.
13. S. C. Lee, E. Sverko, T. Harner, K. Pozo, E. Barresi, J. Schachtshneider, D. Zaruk, M. DeJong and J. Narayan, Retrospective analysis of "new" flame retardants in the global atmosphere under the GAPS network. *Environ. Pollut.*, 2016, **In Press**, <http://dx.doi.org/10.1016/j.envpol.2016.1001.1080>.
14. Y. Yu, H. Hung, N. Alexandrou, P. Roach and K. Nordin, Multiyear measurements of flame retardants and organochlorine pesticides in air in Canada's Western Sub-Arctic. *Environ. Sci. Technol.*, 2015, **49**.
15. EBAS - Database for Atmospheric Composition Research, <http://ebas.nilu.no/>, (accessed March 2016).

16. Y. Su, H. Hung, E. Sverko, P. Fellin and H. Li, Multi-year measurements of polybrominated diphenyl ethers (PBDEs) in the Arctic atmosphere. *Atmos. Environ.*, 2007, **41**, 8725-8735.
17. H. Xiao, L. Shen, Y. S. Su, E. Barresi, M. DeJong, H. L. Hung, Y. D. Lei, F. Wania, E. J. Reiner, E. Sverko and S. C. Kang, Atmospheric concentrations of halogenated flame retardants at two remote locations: The Canadian High Arctic and the Tibetan Plateau. *Environ. Pollut.*, 2012, **161**, 154-161.
18. H. Xiao, H. Hung, F. Wania, R. Lao, E. Sabljic, E. Sverko, Y. D. Lei, P. Fellin and E. Barresi, Field Evaluation of a Flow-Through Sampler for Measuring Pesticides and Brominated Flame Retardants in the Arctic Atmosphere. *Environ. Sci. Technol.*, 2012, **46**, 7669-7676.
19. A. Salamova, M. H. Hermanson and R. A. Hites, Organophosphate and halogenated flame retardants in atmospheric particles from a European Arctic site. *Environ. Sci. Technol.*, 2014, **48**, 6133-6140.
20. R. Bossi, H. Skov, K. Vorkamp, J. Christensen, S. C. Rastogi, A. Egelov and D. Petersen, Atmospheric concentrations of organochlorine pesticides, polybrominated diphenyl ethers and polychloronaphthalenes in Nuuk, South-West Greenland. *Atmos. Environ.*, 2008, **42**, 7293-7303.
21. A. Moller, Z. Y. Xie, R. Sturm and R. Ebinghaus, Polybrominated diphenyl ethers (PBDEs) and alternative brominated flame retardants in air and seawater of the European Arctic. *Environ. Pollut.*, 2011, **159**, 1577-1583.
22. A. Moller, Z. Y. Xie, M. H. Cai, G. C. Zhong, P. Huang, M. G. Cai, R. Sturm, J. F. He and R. Ebinghaus, Polybrominated Diphenyl Ethers vs Alternate Brominated Flame Retardants and Dechloranes from East Asia to the Arctic. *Environ. Sci. Technol.*, 2011, **45**, 6793-6799.